Impulse Strong Mirror Field for High-Energy Particle Handlings

Masakazu Takayama[1,*], Koichi Kindo[2], Akira Matsuo[2], Koushi Kawaguchi[2] and Eiji Nakamura[3-6]

[1]*Akita Prefectural University, 84-4 Ebinokuchi, Tsuchiya, Yurihonjo, Akita 015-0055 Japan*

[2]*The University of Tokyo, the Institute for Solid State Physics (ISSP), 5-1-5 Kashiwanoha, Kashiwa, Chiba 277-8581 Japan*

[3]*High Energy Accelerator Research Organization (KEK), 1-1 Oho, Tsukuba, Ibaraki 305-0801 Japan*

[4]*The Graduate University for Advanced Studies (SOKENDAI), Shonan, Hayama, Kanagawa 240-0193 Japan*

[5]*Tohoku Gakuin University, Faculty of Engineering, 1-13-1 Chuo, Tagajo, Miyagi 985-8537 Japan*

[6]*Tohoku Gakuin University, Research Institute for Engineering and Technology, 1-13-1 Chuo, Tagajo, Miyagi 985-8537 Japan*

Abstract: The technologies for generating strong magnetic flux density of 10 T ~ 1000 T have been developed and become to be utilized for fundamental science studies, especially for solid-state physics. These technologies enable to control the high-energy particles in a compact region, and explore the new frontier of nuclei conversions and nuclear fusion studies. The methods to generate strong mirror field for high-energy particle confinement and handlings are described in this paper.

Keywords: Strong magnetic field, Magnetic mirror, Nuclei conversion, Nuclear fusion, High-energy physics, New particle production.

1. INTRODUCTION

One of the major concerns in the society of the high-energy particle science for wide uses is the development of compact devices to produce a new particle by nuclei conversions [1-5]. Almost all experiments related with nuclei conversion studies in which the primary particles must be energized highly are often performed by high-energy particle accelerators, so the scale of conventional particle accelerators becomes very large. It was too difficult to produce and control high-energy particles in a compact region because the Larmor radius becomes very large (Figure **1**). Nuclei conversion by a compact device requires the confinement of high-energy particles in an effective region. Recently, the techniques of strong magnetic field formation have been developed, called the Mega Gauss technique [6]. 10 ~ 100 T field excitation by using non-destructive coils [7] and 100 ~ 1000 T field excitation by the magnetic flux compression method [8] using revolver type coils are turned to practical use, especially for fundamental studies on solid state physics. A magnetic mirror field or a cusp field is one of the simplest configurations to confine charged particles. There is a possibility of forming the field by the Mega Gauss technique, although it is difficult to make the strong field by a cusp field due to a force-free problem. The example of the model magnet to generate the mirror field and one of the scenarios to generate the strong mirror field over 100 T are described in this paper. The nuclei conversion is expected by highly heating of particles using a pulsed laser into the strong mirror field formed by the Mega Gauss technique.

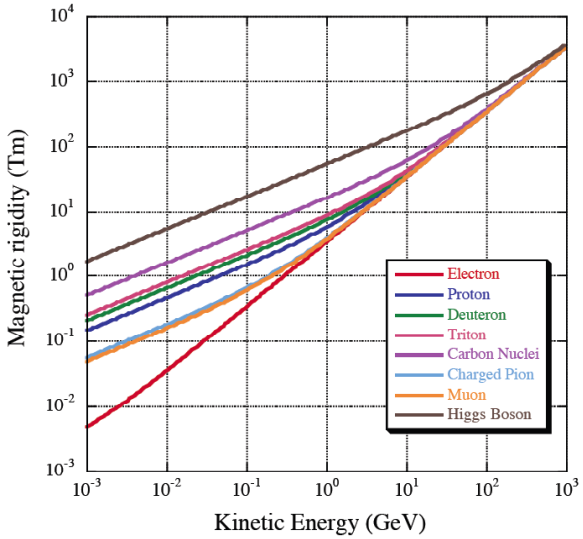

Figure 1: Kinetic energy dependence of magnetic rigidity $B\rho$ for each particle.

*Address correspondence to this author at the Akita Prefectural University, 84-4 Ebinokuchi, Tsuchiya, Yurihonjo, Akita 015-0055 Japan;
Tel: +81 184 27 2089 Fax: +81 184 27 2187; E-mail: masat@akita-pu.ac.jp

E-ISSN: 2408-977X/16

2. STRONG MAGNETIC FIELD EXCITATION BY USING NON-DESTRUCTIVE COILS

A large current excitation is the simplest method to obtain a strong magnetic field. Recent improvements on power supplies enable to generate MA-class large current pulses. The severest problem on the use of the large current pulses is the mechanical breakdown of excitation coils due to the oscillating motion by pulsed electromagnetic force and the heating stress by Joule loss. Figure **2** shows the model magnet assembled for examination of strong magnetic field configuration. The magnet is a split type of solenoids to confirm some possibilities to confine MeV-class particles by mirror field, to bend the orbit of GeV-class particles by Tesla-class circumference field of the magnet, and to undulate electrons to produce photons by synchrotron radiation. The whole magnet assembly is immersed in liquid helium to cool down to 77 K for reducing the resistance of coils from 52 mΩ to 18 mΩ and the Joule heating loss resulting from the reduction of coil resistance. The all components of the magnet assembly are made of non-magnetic materials to avoid unfavorable magnetization. The winding wire is made of mixed materials of 75% copper and 25% silver to improve a mechanical strength. Figure **3** shows the equivalent electric circuit used for the large-current excitation. The power supply is a simple capacitor discharge circuit. Charging to 2.5 mF bank capacitors and switching by two series of ignitrons generate a large current pulse into a magnet throughout high-voltage coaxial cables. The inductance of the magnet L is 177.7 μH and the total amount of resistance is 46 mΩ. The waveforms of the magnetic flux density that are similar to the results from a simulation were measured by use of a small pick-up coil (Figure **4**). Figure **5** shows the excitation linearity of the magnetic flux density measured at the center of the magnet where is the bottom of the mirror field. No unfavorable nonlinear effect was observed. Figure **6** shows the measured magnetic field profile along the longitudinal direction for the charging voltage of 1 kV. The favorable mirror field was formed. The magnetic flux density of 16 T at the bottom and 50 T at the peak (under the solenoid coil) were obtained for the charging voltage of 10 kV, and then the mirror ratio is about 3. Figure **7** shows the measured radial profile of the magnetic flux density at DC low-current excitation to investigate magnetic flux density precisely. The results show that the radial profile is favorable. The residual field was also measured after excitation by 800 A pulsed current with 20 μs half-sine waveform, which is equivalent to 1 T at the peak. From the result, the peak field is 1.5 gauss, which is equivalent to 0.015% of the peak, then that is enough small for handling of high-energy particles.

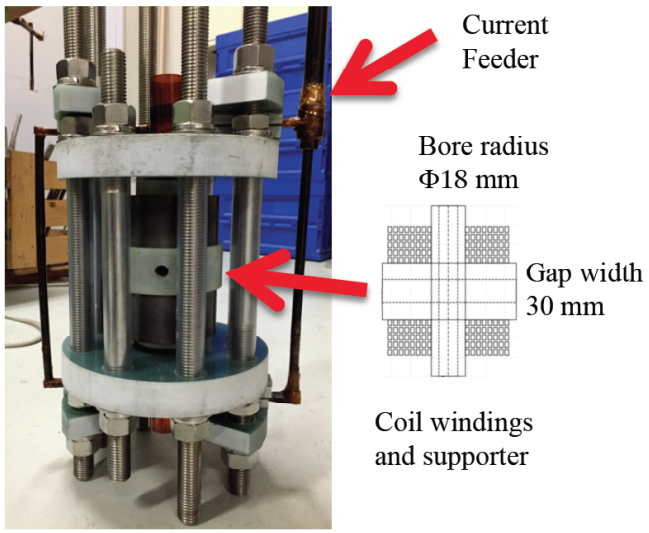

Figure 2: Model magnet assembly of split–type of solenoids.

Table 1: Parameters of the Magnet

Name	Value	Unit
Number of windings	40 (each solenoid)	
Bore diameter	18	mm
Gap width	30	mm

The solenoid coils will be broken by mechanical oscillation and overheating with further current excitation. The boundary condition of the coil being broken is difficult to be defined. The change of magnet inductance is referred as an experiential index. A coil assembly is shrunk slightly due to pulsed electromagnetic force, and then the coil inductance increases slightly. In the other experiments, solenoid coils often were broken when the deviation ratio of magnet inductance $\delta L/L$ reached to 3%. The deviation ratio of the model magnet described in this paper is 1.7% for 50 T excitation (Figure **8**).

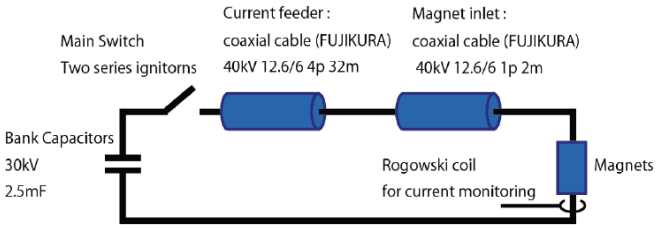

Figure 3: Equivalent electric circuit used for the large-current excitation.

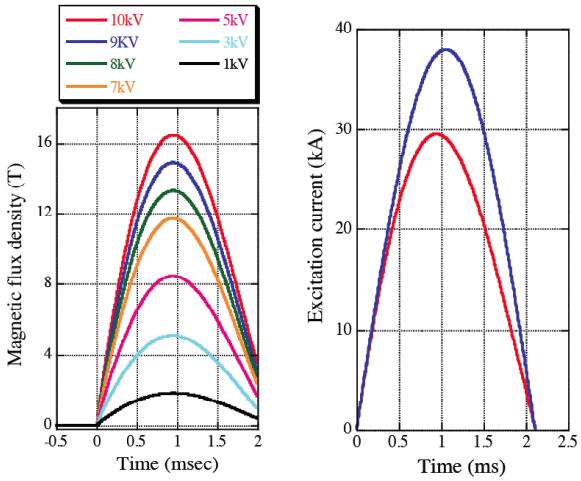

Figure 4: Measured waveforms of magnetic flux density (left) and simulated waveforms of excitation current (right). In the left figure, each measured waveform is obtained for the charging voltages to the capacitor of 1, 3, 5, 7, 8, 9 and 10 kV. In the right figure, the red line shows the measured current waveform and the blue line shows the simulated waveform of the case assumed that the coil has zero-resistance.

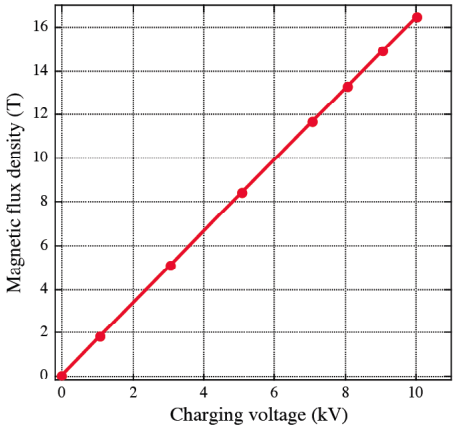

Figure 5: Excitation linearity of magnetic flux density. The horizontal axis indicates the charging voltage. The vertical axis indicates the measured magnetic flux density at the center of the magnet. There was no unfavorable nonlinear effect.

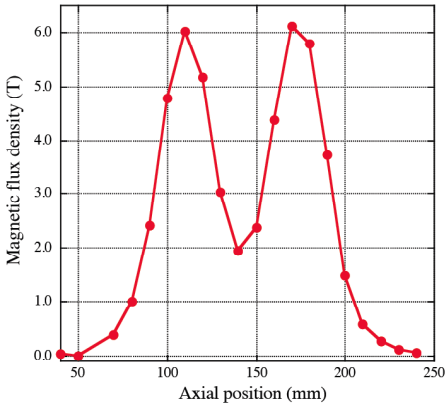

Figure 6: Measured longitudinal magnetic field profile at the charging voltage of 1 kV.

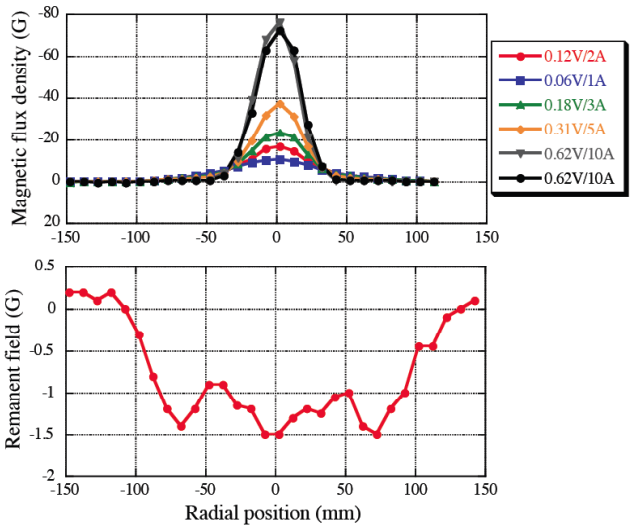

Figure 7: The radial profiles of magnetic flux density. The top figure shows the results of DC-excitation. The bottom figure shows the residual magnetic field.

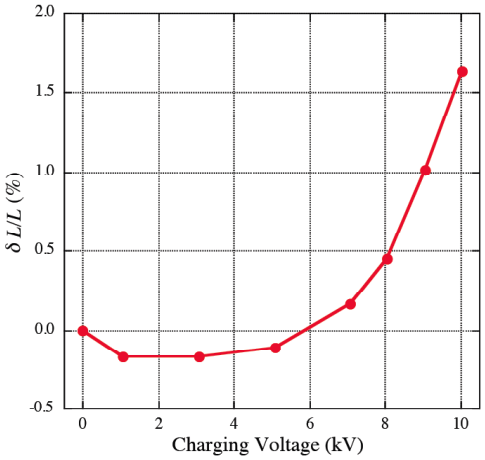

Figure 8: Deviation ratio of magnet inductance $\delta L/L$. The charging voltage of 10 kV generates 50 T at the peak.

3. FURTHER STRONG FIELD BY MAGNETIC FLUX COMPRESSION

Now, a higher magnetic flux density than 100 T can be generated. A high intensity laser [9, 10] can generate more than 20000 T, but the spatial region where the field generated is very small. The laser-driven field technique can generate more than 1000 T in 1-mm region [11], and is expected to generate more than 10000 T, theoretically. It is however difficult to control excitation current stability, so another technique is expected. The flux compression method, which is rather reproducible of more than 100 T field, is described in this paper. The possibility of strong mirror field formation is discussed to show the fundamental scenario by a theoretical approach here.

The fundamental concept of the field compression method is based on the mechanical compression of the inner single-loop coil, called as a liner coil, by the Lorentz force caused by external magnetic field and the eddy current in the liner coil induced by the external time-varying magnetic field. A primary coil generates the pulsed magnetic field for inducting the eddy current in the liner coil (Figure **9**). The liner coil is a cylindrical low-resistance metal pipe and is floated mechanically and electrically from a primary coil. A huge current is induced along the circumferential direction of the cylinder by a time-varying field generated by primary coil current, and then the Lorentz force generated by the induced current and the external magnetic field shrinks the liner coil mechanically. The liner coil keeps a solid body till break down. Then the cross-section of the cylinder increases, the resistance of it decreases and larger current that forms higher magnetic flux density is induced in it. The fundamental prospect can be understood by a simple calculation based on the combined equations of electromagnetic field, equivalent circuit model and a rigid body motion. An example of the time-varying field in a cylindrical symmetry is described here.

A central magnetic field is the sum of an initial external field B_0 (DC component), a primary field B_1(pulsed component) and a field B_2 generated by the liner coil,

$$B = B_0 + B_1 + B_2 . \tag{1}$$

Assuming the liner coil is a rigid body, the radial dependence of the liner coil resistance R can be expressed by the cross-section S, radial position r and those initial values S_0 and r_0, respectively,

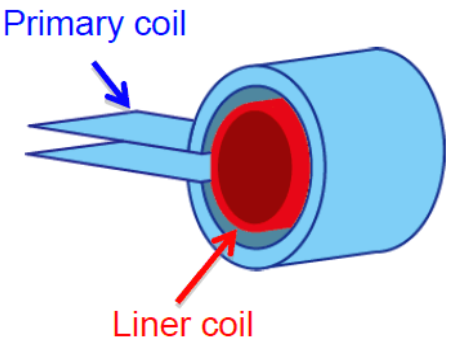

Figure 9: Schematic figure of the coil structure for the field compression method.

$$R \sim \frac{2\pi r\rho}{S} = \frac{2\pi r^2\rho}{rS} = \left(\frac{2\pi\rho}{r_0 S_0}\right) r^2 \tag{2}$$

where ρ is an electrical resistivity of the liner coil material. The cross-section is estimated by

$$S = ld \tag{3}$$

where l and d are the length and the thickness of the liner coil, respectively. The volume $2\pi r/S$ is constant due to a rigid-body condition [12]. The calculation ends at the following condition:

$$r = d/2 = \sqrt{r_0 d_0/2} . \tag{4}$$

the motion of the liner coil is described as follows:

$$\left(B_0 + B_1\right) I_2 = m\frac{d^2 r}{dt^2} - G\left(r - r_0\right) \tag{5}$$

where I_2 is the induced current in the liner coil, m is the mass of the liner coil, and G is the Young's modulus. Each magnetic field is calculated by the Biot-Savart's law and the current in the liner coil can be estimated by the loop voltage V_{loop} induced by the time-varying flux Φ, which produced by the primary coil current. The V_{loop} is written by

$$V_{\text{loop}} \sim -\frac{d\Phi}{dt} = -\frac{d}{dt}\int_0^r \left(B_1 + B_2\right) 2\pi r\, dr$$

$$= -\int_0^r \frac{d\left(B_1 + B_2\right)}{dt} 2\pi r dr - 2\pi r\left(B_1 + B_2\right)\frac{dr}{dt} \tag{6}$$

$$= RI_2 .$$

Every time-varying function can be calculated by Eqs. (1), (2), (5) and (6). Figure **10** shows the example of the calculation results in the case of the parameters

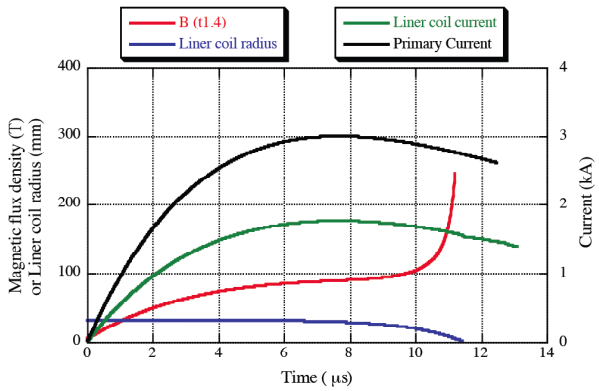

Figure 10: Representative calculation results in the case of the parameters listed in Table **2**. The red line indicates the magnetic flux density. The black line indicates the primary coil current, the green line indicates the induced current in the liner coil, and the blue line indicates the radius of the liner coil.

listed in Table **2**. The field compression can be observed after 8 μs and the magnetic flux density more than 250 T can be expected.

Table 2: Parameters Used for the Calculation

Name	Value	Unit
Primary coil dimension	L100×R40	mm
Liner coil material	Copper	
Young's modulus of Liner coil material	80	GPa
Liner coil initial dimension	L30×R32×t2	mm
Resistivity of liner coil	1.72×10^{-8}	Ωm

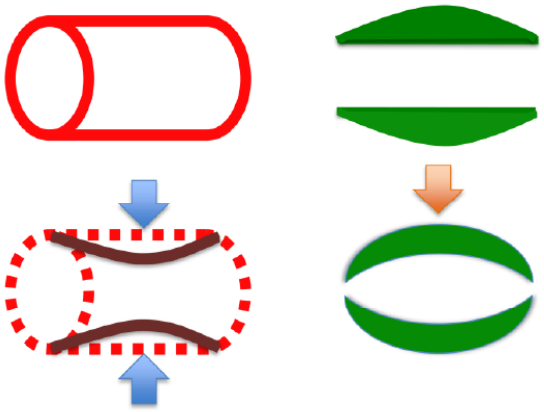

Figure 11: Drawings of shrinks. The shrinking speed at the center would be faster due to the end effect of the cylinder, so mirror field cannot be obtained (left). The shrink speed can be controlled by changing a mechanical strength, for example, changing the thickness of the cylinder as the right figures.

When the liner coil starts to shrink, the shrinking speed at the center would be faster than that at the end due to the end effect of the cylinder, so the mirror field cannot be obtained well (Figure **11** left). On the other hand, changing a mechanical strength, for example, changing the thickness of the cylinder can control the shrink speed, and the mirror field will be obtained (Figure **11** right). Figure **12** shows the example of the magnetic field formed by a distorted ring liner. The distorted ring liner is shrunk by the eddy current induced in it, then it generates a strong mirror field, whereas a flat cylinder generates a divergent magnetic field. There is, therefore, a possibility to form mirror field, as shown in Figures **13** and **14**.

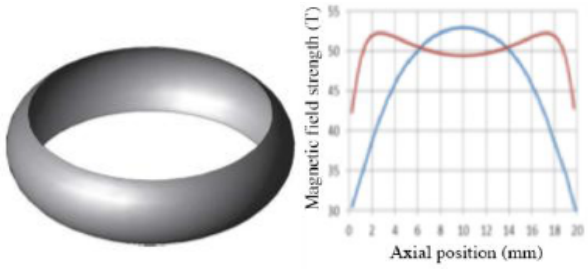

Figure 12: Example of the mirror field formed by a distorted ring liner. The right figure shows the longitudinal magnetic field profile. The red line shows the mirror field when the distorted ring liner (left figure) shrunk. The blue line shows the divergent magnetic field when the flat cylinder shrunk.

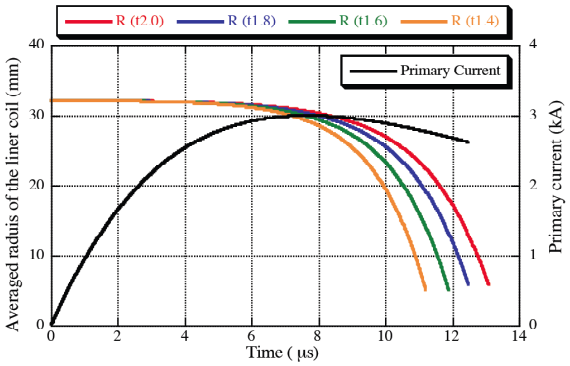

Figure 13: Calculated results of liner coil radius in the four cases for initial thickness of the liner coil of 2.0, 1.8, 1.6 and 1.4 mm.

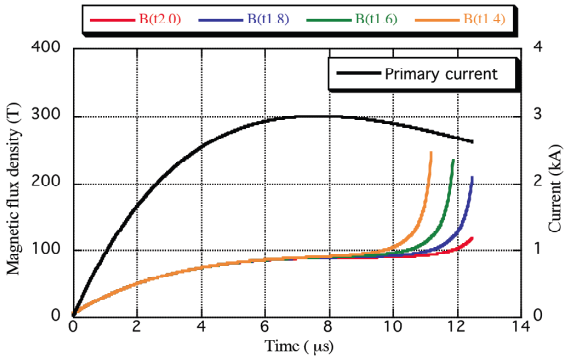

Figure 14: Calculated results of magnetic flux density in the four cases for the initial thickness of the liner coil of 2.0, 1.8, 1.6 and 1.4 mm.

The strong mirror field is the impulse of μs pulse width, but it is sufficient to confine and fuse high-energy particles. It is, of course, expected to form a flat in some time domains by adding a little modulation to a primary excitation current.

SUMMARY

The model magnet with 50 T (at the peak) / 16 T (at the bottom) and the magnetic field compression method are introduced to form a strong mirror field for nuclei conversions. Practical design of the strong mirror field formation will be performed by the simulation using a finite element analysis in the nearest future.

Especially, the time change of the temperature by Joule loss and the like should be deliberated for the precise estimation and design.

ACKNOWLEDGMENTS

We gratefully acknowledge the work of S. Hashimoto. And this work was supported by KAKENHI 21540310, KAKENHI 25286089, KAKENHI 26610074.

REFERENCES

[1] VII: Scientific research symposium on middle range energy production: power supply systems on demand by pulsed operation for nuclear fusion, following conventional fusion methods and using fundamental methods promoted rapidly in this decade, in: Proceedings of the 32nd annual meeting of the Japan Society of Plasma Science and Nuclear Fusion Research, Nagoya Univ., Nagoya, Aichi, Japan, Nov. 27, 2015.

[2] Nakamura E, Future compact fusion reactors using advanced techniques promoted rapidly in this decade, 10th academic meeting combined with nuclear fusion and energy production, 19-134, International congress center, Tsukuba, Japan, June 19th, 2014.

[3] Nakamura E, *et al*., Future compact fusion reactors using advanced techniques promoted rapidly in this decade, Investigative technical committee No. 14-01 in the Japan Society of Plasma Science and Nuclear Fusion Research 2014 (JSPF).

[4] Nakamura E, *et al*., Int J Adv Appl Phys Rec 2015; 2(1): 8. http://dx.doi.org/10.15379/2408-977X.2015.02.01.2

[5] Nakamura E, *et al*., Int J Adv Appl Phys Res 2015; 2(2): 1. http://dx.doi.org/10.15379/2408-977X.2015.02.02.1

[6] International MegaGauss Science Laboratory in Tokyo University.

[7] Kindo Laboratory.

[8] Takeyama Laboratory.

[9] Kitagawa Y and Noda A, J Plasma Fusion 2010; 86(10): 582-588. (written in Japanese)

[10] Nagatomo H, Asahina T, Sano T, Johzaki T, Sunahara A, Sakagami H, *et al.* Laser Driven Implosion in Strong Magnetic field, 10th academic meeting combined with nuclear fusion and energy production, 19-041, International congress center, Tsukuba, Japan, June 19th, 2014.

[11] Successful generation of magnetic fields of 1.5 kilotesla using GEKKO-XII laser - 50 million times that of terrestrial magnetism -, latest research press releases of Osaka University, January 31st, 2013.

[12] KUNIO T. Simulation of the Electromagnetic Flux Compression using LS-DYNA® Multi-Physics Capability, in: Proceedings of 10th European LS-DYNA Conference 2015, Würzburg, Germany.

Received on 18-03-2016 Accepted on 20-05-2016 Published on 30-06-2016

http://dx.doi.org/10.15379/2408-977X.2016.02.04